AIAA SciTech
13-17 January 2014, National Harbor, Maryland
52nd Aerospace Sciences Meeting

A study of the effects of temperature on velocity and density fluctuations in high-subsonic jets

Christophe Bogey*
Laboratoire de Mécanique des Fluides et d'Acoustique
UMR CNRS 5509, Ecole Centrale de Lyon
69134 Ecully, France

The effects of temperature on velocity and density fluctuations in high-subsonic turbulent jets are investigated based on data obtained for one isothermal and three hot jets using compressible Large-Eddy Simulation. The jets have an identical velocity giving an acoustic Mach number $M = u_j/c_a = 0.9$, where subscripts j and a denote inflow and ambient conditions. The isothermal jet is at a diameter-based Reynolds number $Re_D = u_j D/\nu_j = 10^5$. The first two hot jets are at temperatures $T_j = 1.5T_a$ and $T_j = 2.25T_a$, and have the same diameter as the isothermal jet, yielding $Re_D = 5 \times 10^4$ and $Re_D = 2.5 \times 10^4$. The third hot jet is also at $T_j = 1.5T_a$, but its diameter is doubled to maintain $Re_D = 10^5$. Properties of velocity and density fluctuations in the jets, including axial and radial profiles of root-mean-square values and spectra in the shear layers and at the end of the potential core, are presented, and systematically compared with corresponding experimental results. Skewness and kurtosis factors are also shown. As the jet temperature increases, it is found, in particular, that the density shear layer moves outside the velocity shear layer, and that velocity and density fluctuations are stronger around the end of the potential core. In that flow region, the low-frequency content of the velocity spectra is amplified, and the density field displays a high level of intermittency in the hot jets. Finally, preliminary correlations between centerline fluctuations of velocity and density and the near-field pressure are provided for the jet at $T_j = 1.5T_a$ and $Re_D = 10^5$.

I. Introduction

The effects of temperature have been known to be significant on jet noise since the experimental works carried out in the seventies by Fisher *et al.*,[1] Hoch *et al.*[2] and Tanna,[3,4] among others. At an acoustic Mach number of 0.9, a reduction of the overall sound intensity due to heating is observed, but it appears to be negligible at an angle $\phi = 40^o$ relative to the jet direction, and to be progressively larger as ϕ deviates from 40^o. In addition, whereas all acoustic components are weakened at $\phi = 90^o$, a slight increase and a strong decrease of noise levels are visible respectively at low and high frequencies at $\phi = 45^o$, refer to the recent measurements of Bridges *et al.*[5] for instance. The additional components obtained at low frequencies in the jet direction is classically attributed[6] to the creation of extra dipole sources associated with the presence of density fluctuations, which generate noise scaling with the sixth power of the jet velocity.[6–8] This view has been widely accepted, but it was questioned a decade ago by Viswanathan[9] who argued that additional features in sound spectra of hot jets result in some cases from spurious facility noise and/or from Reynolds number effects. A lively and ongoing discussion on that matter has ensued, see the papers by Tester & Morfey,[10] Harper-Bourne,[11] Zaman[12] and Karon & Ahuja.[13]

Identifying the impact of temperature on jet noise generation mechanisms thus remains a challenging task. This is partially attributable to the difficulty in modeling sound sources in turbulent flows unambiguously. This is also due to the fact that a comprehensive description of the velocity and density fields, which is necessary to get a better understanding of aerodynamic sources and entropy sources in hot jets, cannot be easily obtained in experiments. Some trends concerning the influence of temperature on jet flows have

*CNRS Research Scientist, AIAA Senior Member & Associate Fellow, christophe.bogey@ec-lyon.fr

however been established. For instance, Lau[14] found that with rising temperature, the value of the turbulence intensity at the end of the potential core does not vary much, but that its peak value, reached farther downstream, increases. In a series of experiments aimed at exploring aeroacoustic sound sources, Bridges & Wernet,[15,16] Bridges[17] and Panda[18] explored the time-averaged and spectral properties of velocity and density fields in cold and hot jets. Bridges & Wernet remarked[16] that turbulence energy is about ten per cent higher in heated jets than in the unheated case, and that the spectral shapes and two-point space-time correlations of velocity fluctuations are insensitive to temperature if the streamwise location is normalized relative to the potential core length. Using a molecular Rayleigh-scattering technique, Panda[18] noticed that the density shear layer lies on the inside edge of the velocity shear layer in an unheated jet, but on the outside edge in heated jets. Moreover, he also computed cross-correlations between density time series recorded in the jets and pressure time series obtained outside, in order to reveal causal links between the flow and the sound fields.

In order to get new results regarding the influence of temperature on jets, it is now interesting to perform numerical simulations by solving the compressible flow-motion equations,[19–21] which give a direct and simultaneous access to velocity, density and pressure disturbances, and equally to aerodynamic, entropic and acoustic fields. This approach was applied to hot jets a decade ago by Bodony & Lele,[22] who calculated, in particular, centerline root-mean-square (rms) profiles of density fluctuations, and more recently by Bogey & Marsden,[23] who tried to distinguish between temperature effects and Reynolds number effects due to heating. In the latter paper, unfortunately, the jet flow fields were not detailed.

The present work, therefore, aims to investigate the velocity and density fluctuations obtained in the four high-subsonic turbulent jets computed using compressible Large-Eddy Simulation (LES) in Bogey & Marsden.[23] The jets have an identical initial velocity yielding an acoustic Mach number M = 0.9, and Reynolds numbers Re_D between 2.5×10^4 and 10^5. They are characterized, at the exit of a pipe nozzle of radius $r_0 = D/2$, by mean velocity profiles corresponding to a laminar profile of thickness $\delta_0 = 0.15 r_0$, and 9% of peak turbulence intensity. The first jet[24–27] is isothermal, and has a Reynolds number $\mathrm{Re}_D = 10^5$. The first two hot jets are at temperatures $T_j = 1.5 T_a$ and $T_j = 2.25 T_a$, and have the same diameter as the isothermal jet, leading to lower values of Re_D. The third hot jet is also at $T_j = 1.5 T_a$, but its diameter is adjusted in order to maintain $\mathrm{Re}_D = 10^5$. This set of simulations allows temperature effects and Reynolds number effects to be separated. The main objective will be to provide an in-depth description of the velocity and density fluctuations in the jets, in particular in the shear layers and around the end of the potential core, which should lead to the identification of clear trends with heating. Rms values and spectra will be presented, and compared whenever possible with experimental results, especially those given by Bridges & Wernet[15,16] and Panda.[18] In order to examine intermittency in the jets, skewness and kurtosis factors will be also shown. Finally, preliminary correlations between centerline fluctuations of velocity and density and near-field pressure will be provided.

The paper is organized as follows. The main characteristics of the jets and of the simulations, including numerical algorithm and computational parameters, are documented in section II. Properties of velocity and density fluctuations obtained for the different jets are described in section III. Concluding remarks are given in section IV.

II. Parameters

In this section, the jet inflow conditions are presented. The computational parameters are then briefly reported. They are identical to those used in jet simulations which have been thoroughly described in previous references.[24–28] The simulation of the isothermal jet at $\mathrm{Re}_D = 10^5$ considered in the present study was detailed in Bogey *et al.*,[24] in which a great amount of information about the boundary-layer tripping procedure, the discretization quality and the LES reliability is available. The simulations of the hot jets were also reported in Bogey & Marsden.[23]

A. Jet definition

One isothermal and three hot jets at a Mach number $\mathrm{M} = u_j/c_a = 0.9$ are investigated. They originate at $z = 0$ from a pipe nozzle of radius r_0 and length $2r_0$. The ambient temperature and pressure are $T_a = 293$ K and $p_a = 10^5$ Pa. For all jets, the axial velocity profile at the pipe inlet is given by an approximated solution of the Blasius laminar boundary-layer profile. More precisely, a Pohlhausen's fourth-order polynomial profile

of thickness $\delta_0 = 0.15r_0$, and a momentum thickness $\delta_\theta = 0.018r_0$, is imposed.[29] Radial and azimuthal velocities are initially set to zero, pressure is set to p_a, and the temperature is determined by the Crocco-Busemann relation.

In order to generate highly disturbed upstream conditions for the jets, whose initial state would otherwise be laminar, a trip-like forcing is applied to the boundary layers at $z = -0.95r_0$ inside the pipe by adding random low-level vortical disturbances decorrelated in the azimuthal direction. The excitation magnitudes are empirically chosen to obtain, at the pipe exit, mean velocity profiles remaining similar to the Blasius laminar profiles introduced at the pipe inlet, and peak turbulence intensities u'_e/u_j around 9% as in the tripped subsonic jets of Zaman.[30,31] Pressure fluctuations of maximum amplitude 200 Pa random in both space and time are also added in the shear layers from $t = 0$ up to non-dimensional time $t = 12.5r_0/u_j$, in order to speed up the initial transitory period.

The main jet inflow parameters are collected in table 1. Two jet diameters are considered with the aim of distinguishing between the effects of density variations and viscosity variations. The first jet is at ambient temperature, and has a diameter $D = 0.5$ cm giving a Reynolds number $\mathrm{Re}_D = 10^5$. The next two jets are at $T_j = 1.5T_a$ and $T_j = 2.25T_a$, and have the same diameter as the isothermal jet. The two temperatures lead to densities $\rho_j = 0.67\rho_a$ and $\rho_j = 0.44\rho_a$ and to Reynolds numbers $\mathrm{Re}_D = 5 \times 10^4$ and $\mathrm{Re}_D = 2.5 \times 10^4$, respectively. The last jet is also at a temperature of $T_j = 1.5T_a$, but its diameter is doubled in order to obtain $\mathrm{Re}_D = 10^5$ as for the isothermal jet. In this case, the trends observed with heating should correspond to those found experimentally for high-Reynolds-number jets, in which viscosity plays a negligible role.

Table 1. Jet parameters: Mach number $\mathrm{M} = u_j/c_a$, temperature T_j, diameter D, Reynolds number $\mathrm{Re}_D = u_j D/\nu_j$, density ρ_j, nozzle-exit boundary-layer momentum thickness $\delta_\theta(0)$ and peak turbulence intensity u'_e/u_j, and potential core length z_c (subscripts j and a denote inflow and ambient conditions, respectively).

M	T_j/T_a	D (cm)	Re_D	ρ_j/ρ_a	$\delta_\theta(0)/r_0$	u'_e/u_j	z_c/r_0
0.9	1	0.5	10^5	1	0.0185	9.18%	15.9
0.9	1.5	0.5	5×10^4	0.67	0.0191	9.14%	12.5
0.9	2.25	0.5	2.5×10^4	0.44	0.0200	9.17%	10.6
0.9	1.5	1	10^5	0.67	0.0185	9.15%	13.2

In order to illustrate the jet initial conditions, the profiles of mean and rms axial velocity calculated at the nozzle exit are represented in figures 1(a-b), and the main exit flow parameters are provided in table 1. As intended, the mean velocity profiles do not appreciably differ from the Blasius laminar profile imposed at the pipe-nozzle inlet, leading to boundary-layer momentum thicknesses $\delta_\theta(0) = 0.0185r_0 - 0.02r_0$, and the turbulence intensity profiles closely resemble each other, all reaching a peak around $u'_e/u_j = 9.15\%$. The profiles are also shown to be comparable to those measured by Zaman[30,31] in a tripped jet at $\mathrm{Re}_D = 10^5$. These results indicate that the jets are initially highly disturbed but not fully turbulent, and that they are characterized by similar nozzle-exit conditions except for the temperature and the Reynolds number.

B. LES procedure and numerical methods

The LES are carried out using a solver of the three-dimensional filtered compressible Navier-Stokes equations in cylindrical coordinates (r, θ, z) based on low-dissipation and low-dispersion explicit schemes. The axis singularity is taken into account by the method of Mohseni & Colonius.[32] In order to alleviate the time-step restriction near the cylindrical origin, the derivatives in the azimuthal direction around the axis are calculated at coarser resolutions than permitted by the grid.[33] Fourth-order eleven-point centered finite differences are used for spatial discretization, and a second-order six-stage Runge-Kutta algorithm is implemented for time integration.[34] A sixth-order eleven-point centered filter[35] is applied explicitly to the flow variables every time step. Non-centered finite differences and filters are used near the pipe walls and the grid boundaries.[29,36] The radiation conditions of Tam & Dong[37] are applied at all boundaries, with the addition at the outflow of a sponge zone combining grid stretching and Laplacian filtering.[38]

In the simulations, the explicit filtering is employed to remove grid-to-grid oscillations, but also as a subgrid high-order dissipation model to relax turbulent energy from scales at wave numbers close to the grid cut-off wave number while leaving larger scales mostly unaffected.[39–41] With this in mind, the reliability of the LES fields obtained for the isothermal jet of the present study has been assessed in Bogey *et al.*[24] based on the tranfer functions associated with molecular viscosity, relaxation filtering and time integration.

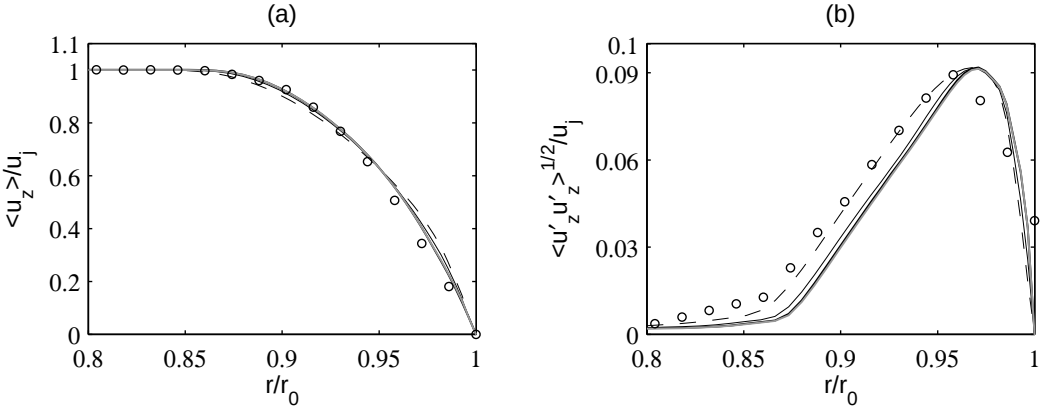

Figure 1. Profiles at $z = 0$ (a) of mean axial velocity $< u_z >$ and (b) of the rms values of axial velocity fluctuations u'_z for: ——— $T_j = T_a$ and $\mathrm{Re}_D = 10^5$, ——— $T_j = 1.5T_a$ and $\mathrm{Re}_D = 5 \times 10^4$, – – – $T_j = 2.25T_a$ and $\mathrm{Re}_D = 2.5 \times 10^4$, ——— $T_j = 1.5T_a$ and $\mathrm{Re}_D = 10^5$; ∘ measurements of Zaman[30,31] for a tripped jet at $\mathrm{Re}_D = 10^5$ about $0.1r_0$ downstream of the exit plane.

Viscosity was shown to be the dominant dissipation mechanism for scales discretized at least by seven points per wavelength. The physics of the larger turbulent structures is therefore not likely to be governed by numerical or subgrid-modeling dissipation. This allows in particular the effective flow Reynolds number not to be artificially decreased, and viscosity effects to be properly captured, as was the case in Bogey *et al.*[24] for isothermal jets at Re_D between 2.5×10^4 and 2×10^5. These remarks certainly equally hold in this work for the LES of the hot jets which are at Reynolds numbers equal to or lower than that of the isothermal jet.

C. Simulation parameters

As indicated in table 2, the LES are performed using a grid containing $n_r \times n_\theta \times n_z = 252$ million points. There are 169 points along the pipe nozzle, 77 points within the jet radius, and 31 points inside the inlet boundary layers. The physical domain, excluding the eighty-point outflow sponge zone, extends axially down to $L_z = 25r_0$, and radially out to $L_r = 9r_0$.

Table 2. Simulation parameters: numbers of grid points n_r, n_θ and n_z, mesh spacings Δr at $r = r_0$, $r_0\Delta\theta$, and Δz at $z = 0$, extents L_r and L_z of the physical domain, number of time steps n_{it} and time duration T ($^*n_{it} = 140,000$ and $Tu_j/r_0 = 320$ for the jet at $T_j = 1.5T_a$ and $\mathrm{Re}_D = 10^5$).

$n_r \times n_\theta \times n_z$	$\Delta r/r_0$	$r_0\Delta\theta/r_0$	$\Delta z/r_0$	L_r, L_z	n_{it}	Tu_j/r_0
$256 \times 1024 \times 962$	0.36%	0.61%	0.72%	$9r_0, 25r_0$	164,000*	375*

The mesh spacing is uniform in the azimuthal direction, with $r_0\Delta\theta = 0.0061r_0$. In the axial direction, the mesh spacing is minimum between $z = -r_0$ and $z = 0$, with $\Delta z = 0.0072r_0$. It increases upstream of $z = -r_0$, but also downstream of the nozzle at stretching rates lower than 1% allowing to reach $\Delta z = 0.065r_0$ between $z = 13.3r_0$ and $z = L_z = 25r_0$. In the radial direction, the mesh spacing is minimum around $r = r_0$, with $\Delta r = 0.0036r_0$. It is equal to $\Delta r = 0.292r_0$ close to the jet axis, to $\Delta r = 0.081r_0$ between $r = 3r_0$ and $r = 6.75r_0$, and finally to $\Delta r = 0.176r_0$ at $r = L_r = 9r_0$.

The grid quality has been discussed in Bogey *et al.*[24] for the isothermal jet of the present study. The ratios between the integral length scales of the axial fluctuating velocity and the mesh spacings along the lip line were shown to fall between 4 and 10. The properties of the nozzle-exit turbulence and of the shear-layer flow fields were moreover found to be practically converged with respect to the grid. Based on these results, there seems little doubt that the grid resolution is also appropriate for the three hot jets, whose Reynolds numbers are the same as or lower than that of the isothermal case. Indeed, lower Reynolds numbers lead to an increase of the integral length scales and to the weakening of fine-scale turbulence.[27]

The simulation time T, given in table 2, is equal to $320r_0/u_j$ for the jet at $T_j = 1.5T_a$ and $\mathrm{Re}_D = 10^5$, and to $375r_0/u_j$ for the three others. After the initial transitory period, from $t = 100r_0/u_j$ onwards, density, velocity components and pressure are recorded along the jet axis, and on two surfaces at $r = r_0$ and $r = 6.5r_0$, at a sampling frequency allowing spectra to be computed up to a Strouhal number of

$\mathrm{St}_D = fD/u_j = 20$, where f is the time frequency. The radial mesh spacing at $r = 6.5r_0$ yields a Strouhal number of $\mathrm{St}_D = fD/u_j = 6.9$ for an acoustic wave discretized by four points per wavelength. In the azimuthal direction, every fourth grid point is stored. The velocity and density spectra are evaluated from overlapping samples of duration $27.4r_0/u_j$. The flow statistics are determined from $t = 175r_0/u_j$ onwards, and they are averaged in the azimuthal direction.

The simulations have run using an OpenMP-based in-house solver, on 7 processors of a NEC SX-8 computer at a central processing unit (CPU) speed of around 36 Gflops, then on 32 processors of an IBM Power7 computer. For 100,000 time steps, 4,200 CPU core hours and 66,000 CPU core hours were required, respectively. About 60 GB of memory were necessary.

III. Results

A. Velocity and density fluctuation snapshots

Snapshots of velocity and density fluctuations obtained in the four jets are represented in figures 2(a-d) and 3(a-d), respectively. As noticed previously,[23] the velocity fields are seen to develop more rapidly with increasing temperature. This leads to a shorter potential core, compare for instance figures 2(a) and 2(c), ending at $z_c = 15.9r_0$ for $T_j = T_a$, $z_c \simeq 13r_0$ for $T_j = 1.5T_a$, and $z_c = 10.6r_0$ for $T_j = 2.25T_a$, as reported in table 1. The fluctuating velocity fields however appear to have similar structures in the isothermal jet and in the hot jets. In all cases, they are dominated by large scales, which can most probably be related to coherent turbulent structures.

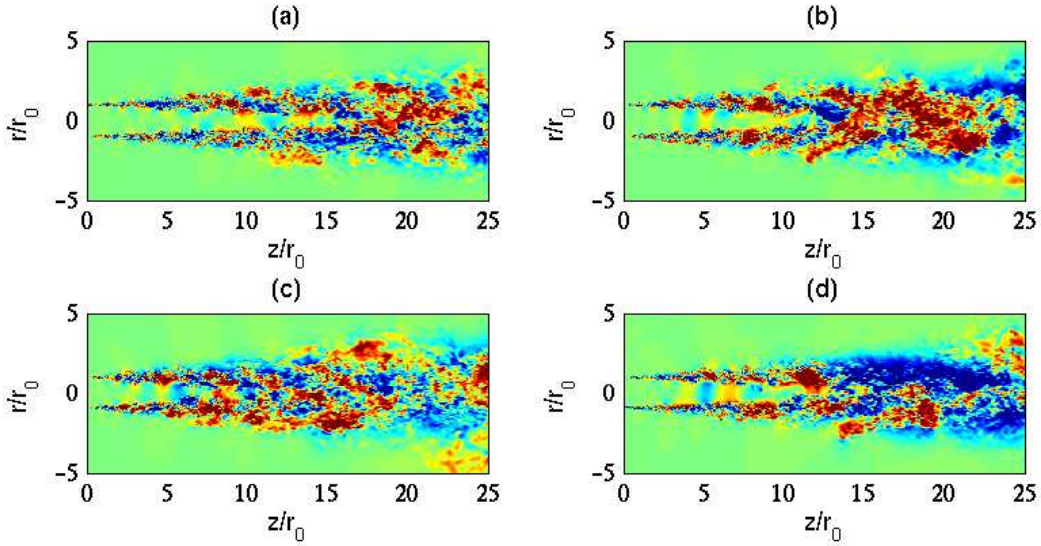

Figure 2. Snapshots in the (z, r) plane of axial velocity fluctuations u'_z for: (a) $T_j = T_a$ and $\mathrm{Re}_D = 10^5$, (b) $T_j = 1.5T_a$ and $\mathrm{Re}_D = 5 \times 10^4$, (c) $T_j = 2.25T_a$ and $\mathrm{Re}_D = 2.5 \times 10^4$, (d) $T_j = 1.5T_a$ and $\mathrm{Re}_D = 10^5$. The color scale ranges from $-0.18u_j$ up to $0.18u_j$.

On the contrary, in figure 3, the density fields look quite different in the isothermal jet and in the hot jets. The most significant density fluctuations are located along the lip line in the velocity shear layers in the isothermal case, but outside the shear layers in the three hot cases. They seem also to be characterized by coherent large scales in the former case, as was found for the velocity fluctuations, but by finer scales in the latter.

B. Velocity and density fluctuations in the shear layers

The variations between $z = 0$ and $z = 10r_0$ of the peak rms values of axial and radial velocity fluctuations u'_z and u'_r are displayed in figures 4(a-b). For the jets at a constant diameter, with rising temperature, a hump progressively emerges around $z = 2r_0$ in the profiles of turbulence intensities. Consequently, the peak values increase, and are equal, at the three temperatures considered, to 15.4%, 17.1% and 18.6% for u'_z and 11.2%, 12.7% and 14% for u'_r. For the two jets at $\mathrm{Re}_D = 10^5$, the profiles look, on the contrary, very much alike. In

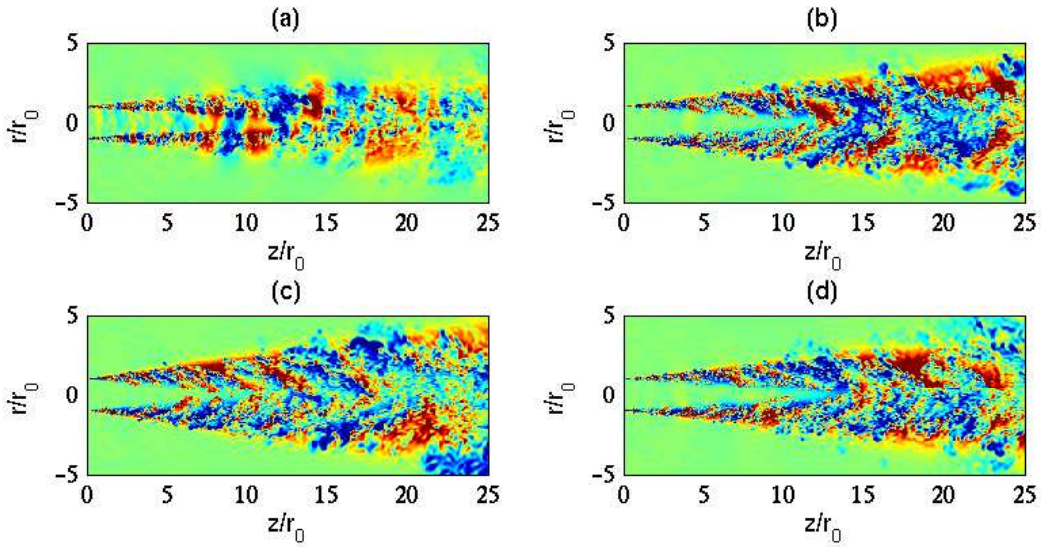

Figure 3. Snapshots in the (z, r) plane of density fluctuations ρ' for: (a) $T_j = T_a$ and $\mathrm{Re}_D = 10^5$, (b) $T_j = 1.5T_a$ and $\mathrm{Re}_D = 5 \times 10^4$, (c) $T_j = 2.25T_a$ and $\mathrm{Re}_D = 2.5 \times 10^4$, (d) $T_j = 1.5T_a$ and $\mathrm{Re}_D = 10^5$. The color scales range from $-0.024\rho_a$ up to $0.024\rho_a$ in the first case, and from $-0.21(\rho_a - \rho_j)$ up to $0.21(\rho_a - \rho_j)$ in the others.

this case, heating results in a slight increase of the fluctuation levels, yielding, at $T_j = 1.5T_a$, maximum rms values of $0.16u_j$ for u'_z and $0.116u_j$ for u'_r. The strengthening of the peak turbulence intensities in the jets with the same diameter can therefore be attributed to Reynolds number effects.[27] It can finally be noted that at large distances from the nozzle, typically for $z > 8r_0$, the levels of velocity fluctuations are ordered by the temperature. This is true for instance in figure 4(a), where the rms velocity values at $z = 10r_0$ are found to be of 14.8% at $T_j = T_a$, 15.6% at $T_j = 1.5T_a$ and $\mathrm{Re}_D = 10^5$, 15.7% at $T_j = 1.5T_a$ and $\mathrm{Re}_D = 5 \times 10^4$, and 16.4% at $T_j = 2.25T_a$. This tendency, which will be discussed in the next section, is consistent with the experimental data obtained by Bridges & Wernet[16] for unheated and heated jets with the same velocity.

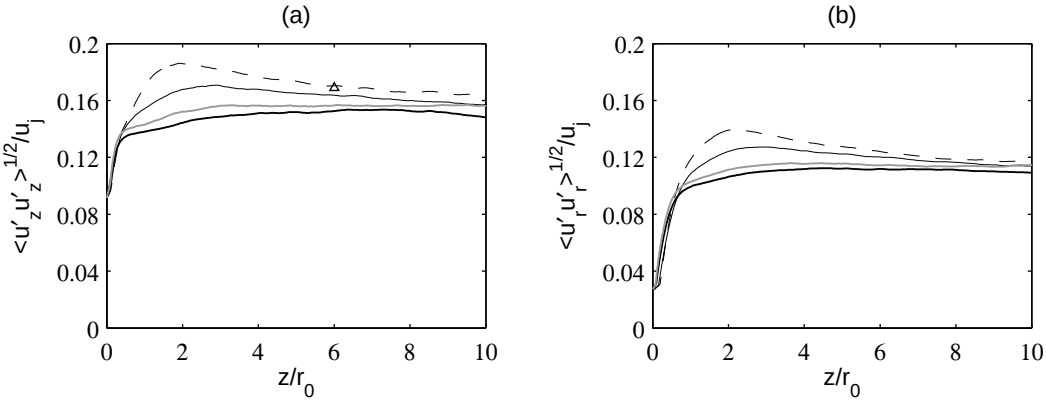

Figure 4. Variations of peak rms values of velocity fluctuations (a) u'_z and (b) u'_r for: ——— $T_j = T_a$ and $\mathrm{Re}_D = 10^5$, ——— $T_j = 1.5T_a$ and $\mathrm{Re}_D = 5 \times 10^4$, – – – $T_j = 2.25T_a$ and $\mathrm{Re}_D = 2.5 \times 10^4$, ——— $T_j = 1.5T_a$ and $\mathrm{Re}_D = 10^5$; △ measurement of Bridges & Wernet[15] for a M = 0.9 jet with $D = 5.1$ cm at $T_j = 1.82T_a$.

Spectra of the radial velocity u'_r are computed at $r = r_0$ on the lip line at two axial locations $z = r_0$ and $z = 6r_0$. They are presented in figures 5(a-b) as a function of the Strouhal number St_D. At the first location, in figure 5(a), the spectra obtained for the two jets at the same $\mathrm{Re}_D = 10^5$ but at different T_j nearly superimpose, confirming that the development of the mixing layer immediately downstream of the nozzle essentially depends on the Reynolds number. For the jets of identical diameter, increasing temperature thus leads to the narrowing of the velocity spectra and the emergence of an instability-like component, as was the case for isothermal jets at decreasing Reynolds numbers.[27] This component is found around $\mathrm{St}_D = 1.4$,

yielding $\mathrm{St}_\theta = f\delta_\theta/u_j \simeq 0.013$, which corresponds to the frequencies predominating early on in initially laminar annular mixing layers.[42,43] Farther downstream at $z = 6r_0$, in figure 5(b), the spectra obtained for the two jets at $T_j = 1.5T_a$ but various Re_D are, on the contrary, close to one another, indicating that temperature is the key parameter here. In this case, an elevated temperature results in velocity spectra of the same shape with slightly higher amplitude. This is in agreement with the measurements of Bridges & Wernet[16] in the mixing layers of jets at axial positions equal to half the potential core length.

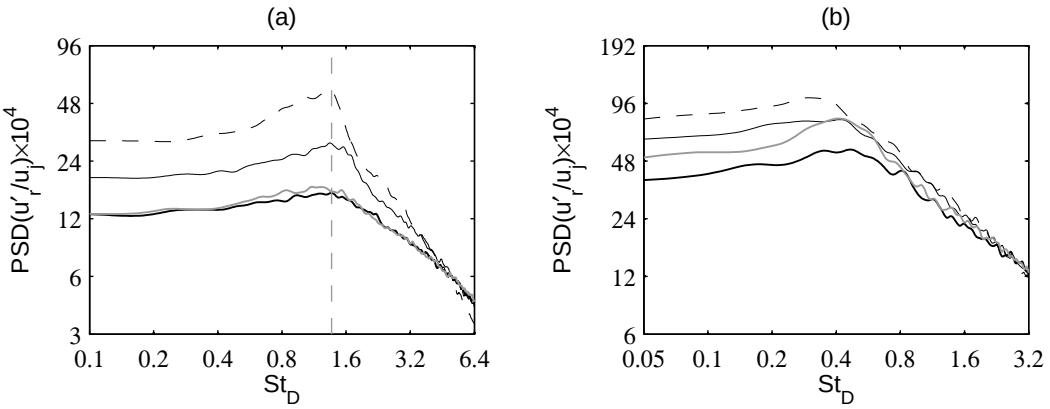

Figure 5. Power spectral densities (PSD) of radial velocity fluctuations u'_r at $r = r_0$, (a) at $z = r_0$ and (b) at $z = 6r_0$, as functions of $\mathrm{St}_D = fD/u_j$, for: ——— $T_j = T_a$ and $\mathrm{Re}_D = 10^5$, ——— $T_j = 1.5T_a$ and $\mathrm{Re}_D = 5 \times 10^4$, – – – $T_j = 2.25T_a$ and $\mathrm{Re}_D = 2.5 \times 10^4$, ——— $T_j = 1.5T_a$ and $\mathrm{Re}_D = 10^5$; – – – frequency given by $\mathrm{St}_\theta = f\delta_\theta/u_j = 0.013$ for $\delta_\theta = 0.019r_0$.

The variations between $z = 0$ and $z = 10r_0$ of the peak rms values of density ρ' normalized by ρ_a and $|\rho_j - \rho_a|$ are presented in figures 6(a-b). In figure 6(a), the levels of density fluctuations are found to increase with the jet temperature, as expected. When non-dimensionalized by $|\rho_j - \rho_a|$, in figure 6(b), the curves obtained for the hot jets however show strong similarities. They reach a peak very near to the nozzle exit, which seems not to depend on temperature, but to occur more rapidly and to be more pronounced at higher Reynolds numbers. Farther downstream, a progressive decrease with the axial distance is observed, and the rms values of density are remarkably close in the three jets. With respect to the values measured by Panda[18] at $z = 6z_0$ in jets with diameter $D = 5.1$ cm at $T_j = 1.82T_a$ and $T_j = 2.7T_a$, they appear slightly higher, which may be due to Reynolds number effects.

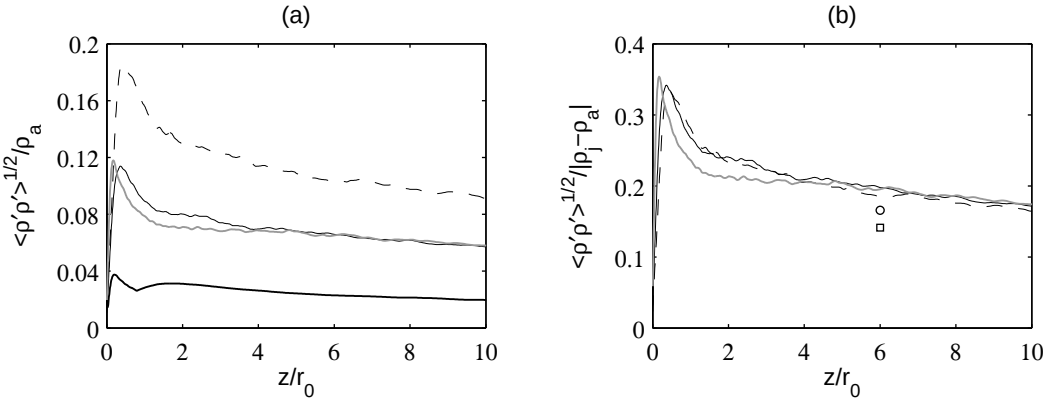

Figure 6. Variations of peak rms values of density fluctuations ρ', normalized (a) by ρ_a and (b) by $|\rho_j - \rho_a|$, for: ——— $T_j = T_a$ and $\mathrm{Re}_D = 10^5$, ——— $T_j = 1.5T_a$ and $\mathrm{Re}_D = 5 \times 10^4$, – – – $T_j = 2.25T_a$ and $\mathrm{Re}_D = 2.5 \times 10^4$, ——— $T_j = 1.5T_a$ and $\mathrm{Re}_D = 10^5$; measurements of Panda[18] for M = 0.9 jets with $D = 5.1$ cm: □ $T_j = 1.82T_a$, ○ $T_j = 2.7T_a$.

Spectra of density ρ' non-dimensionalized by $|\rho_j - \rho_a|$ are calculated on the lip line at $z = 0.5r_0$ and $z = 6r_0$ for the hot jets. They are plotted in figures 7(a-b) as a function of the Strouhal number St_D. At the first axial position, in figure 7(a), the spectra are dominated by components around $\mathrm{St}_D = 1.4$, corresponding to the frequency emerging in the velocity spectra during the early stage of mixing-layer development, see in

figure 5(a). They also appear to depend mainly on the jet Reynolds number, and to broaden with increasing Re_D. In particular, there is no significant amplification of the low-frequency content with heating, which is in contradiction with measurements made by Panda[18] at the same position in heated jets. As for the density spectra determined at $z = 6r_0$, in figure 7(b), they are found not to change appreciably either with the Reynolds number or, contrarily to the velocity spectra of figure 5(b), with the jet temperature. They are in very good agreement with a spectrum obtained by Panda[18] at almost the same location in a M = 0.9 jet at $T_j = 1.82T_a$.

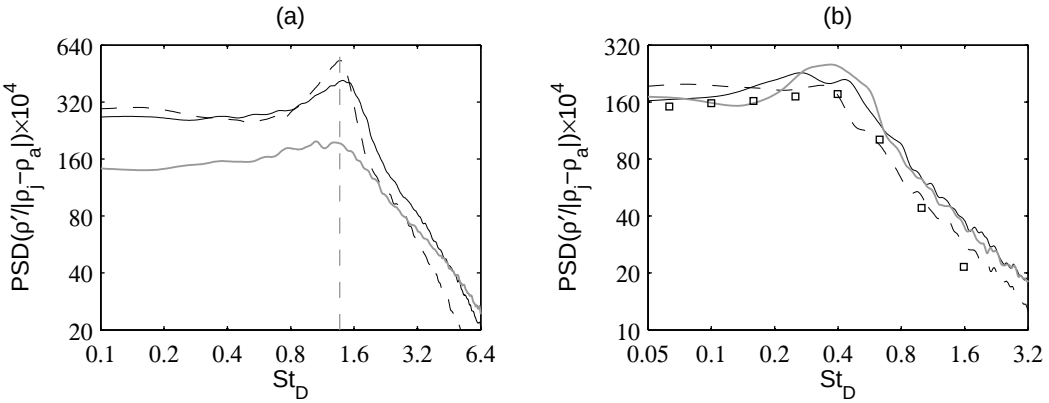

Figure 7. Power spectral densities (PSD) of density fluctuations ρ' at $r = r_0$, (a) at $z = 0.5r_0$ and (b) at $z = 6r_0$, as functions of St_D, for: ——— $T_j = 1.5T_a$ and $\mathrm{Re}_D = 5 \times 10^4$, − − − $T_j = 2.25T_a$ and $\mathrm{Re}_D = 2.5 \times 10^4$, ——— $T_j = 1.5T_a$ and $\mathrm{Re}_D = 10^5$; – – – frequency given by $\mathrm{St}_\theta = f\delta_\theta/u_j = 0.013$ for $\delta_\theta = 0.019r_0$; □ measurements of Panda[18] at $r = 1.08r_0$ and $z = 6r_0$ for a M = 0.9 jet with $D = 5.1$ cm at $T_j = 1.82T_a$.

The radial distributions of the rms values of velocity and density fluctuations are compared at $z = 6r_0$ in figures 8(a-b). They are seen to agree reasonably well with data provided by Bridges & Wernet[15] and Panda[18] for hot jets. Above all, the shapes of the profiles exhibit clear differences depending on whether velocity or density is considered, and whether the jet is heated. For velocity, in figure 8(a), the rms profiles in the isothermal jet and in the hot jets are closely matching, all reaching a maximum around $r = 0.9r_0$. For density, in figure 8(b), this is not true, and the rms profile moves to the inner side of the shear layer for the isothermal jet and, inversely, to the outer side for the hot jets, with peaks observed at $r \simeq 0.8r_0$ and $r \simeq 1.3r_0$, respectively. Besides, the profiles estimated in the hot cases, normalized by $|\rho_j - \rho_a|$, are quite similar, and therefore do not vary much with temperature. These results nicely follow and support the trends identified by Panda[18] for cold and heated jets. As pointed out by the author above, they may be of interest for turbulence and noise source modelling.

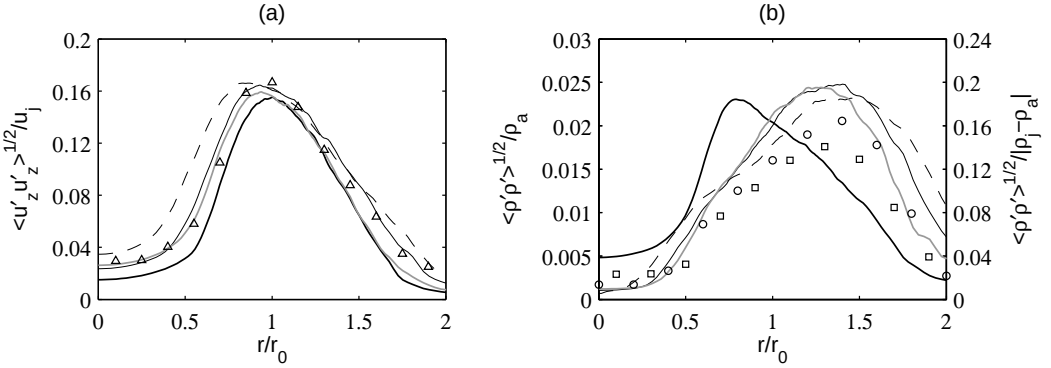

Figure 8. Radial profiles at $z = 6r_0$ of the rms values of (a) velocity fluctuations u'_z and (b) density fluctuations ρ' for: ——— $T_j = T_a$ and $\mathrm{Re}_D = 10^5$, ——— $T_j = 1.5T_a$ and $\mathrm{Re}_D = 5 \times 10^4$, − − − $T_j = 2.25T_a$ and $\mathrm{Re}_D = 2.5 \times 10^4$, ——— $T_j = 1.5T_a$ and $\mathrm{Re}_D = 10^5$; measurements of Bridges & Wernet[15] and Panda[18] for M = 0.9 jets with $D = 5.1$ cm: △ and □ $T_j = 1.82T_a$, ○ $T_j = 2.7T_a$. In right figure, the rms values of density are normalized by ρ_a for the isothermal jet, and by $|\rho_j - \rho_a|$ for the others.

Finally, the skewness and kurtosis factors of the axial velocity and density fluctuations are calculated in order to quantify the intermittency of the phenomena taking place in the shear layers. The radial profiles

obtained at $z = 6r_0$ for the velocity are presented in figure 9(a-b). Their shapes are similar in the isothermal jet and in the hot jets. In all cases, significant values are observed between the turbulent shear layers and the laminar regions, namely the potential core and the flow surrounding the jet. The skewness factors exhibit large negative values at $r \simeq 0.6r_0$ around the inner side of the shear layer, and large positive values at $r \simeq 2r_0$ around the outer side, which most probably result from burts of low- and high-velocity fluid in these two zones, respectively. Moreover, with rising jet temperature, the values of skewness and kurtosis do not change much in the inner region, but increase in the outer region.

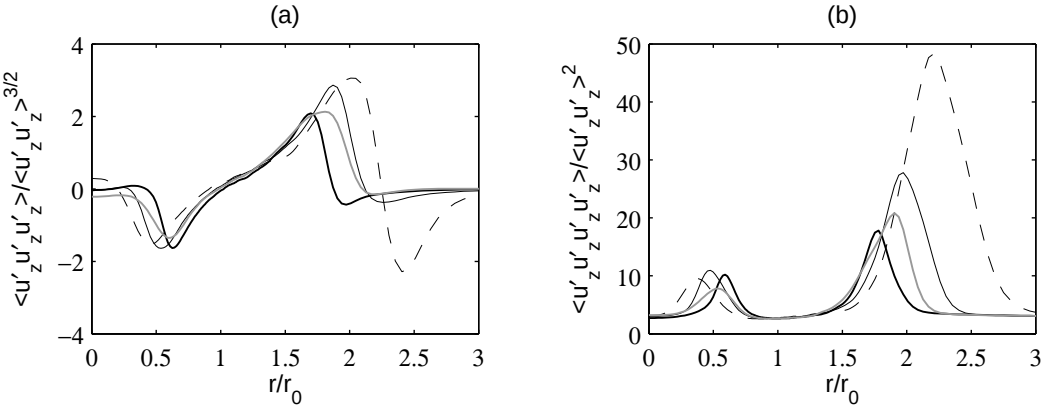

Figure 9. Radial profiles at $z = 6r_0$ of (a) the skewness and (b) the kurtosis factors of of velocity fluctuations u'_z for: ——— $T_j = T_a$ and $\mathrm{Re}_D = 10^5$, ——— $T_j = 1.5T_a$ and $\mathrm{Re}_D = 5 \times 10^4$, − − − $T_j = 2.25T_a$ and $\mathrm{Re}_D = 2.5 \times 10^4$, ——— $T_j = 1.5T_a$ and $\mathrm{Re}_D = 10^5$.

The radial profiles of skewness and kurtosis factors obtained at $z = 6r_0$ for the density fluctuations are shown in figure 10(a-b). Small values are found in the isothermal jet, whereas very large values are observed in the hot jets, indicating weak intermittency in the former case, but strong intermittency in the latter. In the hot jets, positive and negative values of skewness are found around the inner and outer sides of the shear layer, respectively, which can be attributed to the intrusion of high-density (cold) fluid and low-density (hot) fluid in these two regions. The kurtosis factors, hence intermittency, also appear to increase with the temperature.

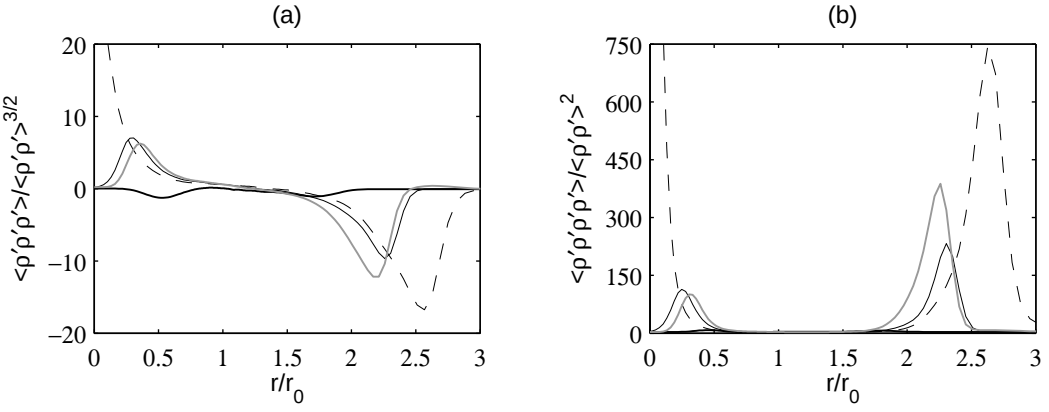

Figure 10. Radial profiles at $z = 6r_0$ of (a) the skewness and (b) the kurtosis factors of of density fluctuations ρ' for: ——— $T_j = T_a$ and $\mathrm{Re}_D = 10^5$, ——— $T_j = 1.5T_a$ and $\mathrm{Re}_D = 5 \times 10^4$, − − − $T_j = 2.25T_a$ and $\mathrm{Re}_D = 2.5 \times 10^4$, ——— $T_j = 1.5T_a$ and $\mathrm{Re}_D = 10^5$.

C. Velocity and density fluctuations in the jets

The variations of the centerline rms values of axial and radial fluctuating velocities are displayed in figures 11(a-b). The temperature effects turn out to be stronger than the Reynolds number effects. With rising temperature, the peak turbulence intensities are reached at axial locations farther upstream, as expected given the shortening of the jet potential core, and they increase appreciably. They are equal to 11.4% at

$T_j = T_a$, about 13.3% at $T_j = 1.5T_a$, and 14.6% at $T_j = 2.25T_a$ for velocity u'_z, Similar trends were observed in the experiments of Lau,[14] Lepicovsky,[44] Kearney-Fischer *et al.*,[45] and Bridges.[17] The latter author obtained, on the centerline of Mach number 0.9 jets, peak levels of axial velocity fluctuations varying from 14.8% of u_j at $T_j = 0.84T_a$ to 15.6% of u_j at $T_j = 1.76T_a$. These values do not match well those found in the present study, which may be due to different jet initial conditions. This is also not surprising in view of the significant dispersion of the measurements of turbulence intensities in jets, compare for instance the experimental data of Fleury *et al.*[46] and of Arakeri *et al.*[47] in figures 11(a-b).

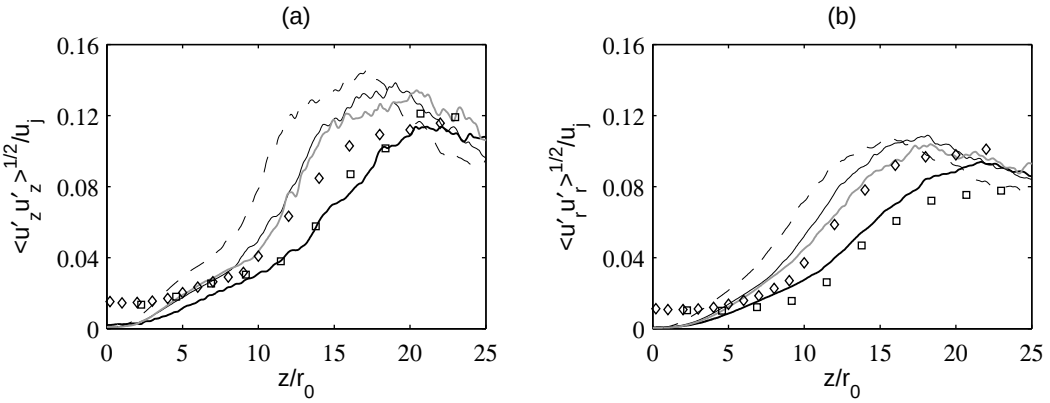

Figure 11. Centerline variations of rms values of velocity fluctuations (a) u'_z and (b) u'_r for: ——— $T_j = T_a$ and $\mathrm{Re}_D = 10^5$, ——— $T_j = 1.5T_a$ and $\mathrm{Re}_D = 5 \times 10^4$, – – – $T_j = 2.25T_a$ and $\mathrm{Re}_D = 2.5 \times 10^4$, ——— $T_j = 1.5T_a$ and $\mathrm{Re}_D = 10^5$; measurements for M = 0.9 jets at $\mathrm{Re}_D \geq 4 \times 10^5$: ◇ $T_j = T_a$ (from Fleury *et al.*[46]), □ $T_j = 1.1T_a$ (from Arakeri *et al.*[47]).

Spectra of velocity u'_z are calculated at $z = z_c$ at the end of the potential core, which is a region of special interest in subsonic jets concerning noise sources radiating in the downstream direction according, in particular, to flow-acoustic correlation studies.[48,49] The spectra obtained at $r = 0$ on the jet axis and at $r = r_0$ on the lip line are presented in figures 12(a-b) as a function of St_D, and compared with measurements of Bridges & Wernet[16] for M = 0.9 jets at $T_j = 0.84T_a$ and $T_j = 1.76T_a$. Numerical and experimental results are very similar, and exhibit the same trends. With rising temperature, in general, the shape of the spectra does not vary much, but their amplitude becomes higher. Looking in more detail, however, the impact of temperature is more important on the jet axis than on the lip line. At $r = 0$, in figure 12(a), the levels of velocity fluctuations grow strongly for $\mathrm{St}_D \leq 0.6$, but do not change appreciably for $\mathrm{St}_D \geq 0.6$. As a result, the peak components shift to lower Strouhal numbers, from $\mathrm{St}_D \simeq 0.3$ for the isothermal jet down to $\mathrm{St}_D \simeq 0.2$ for the jet at $T_j = 2.25T_a$. In comparison, at $r = r_0$, the increase in amplitude with heating is less marked, especially at low frequencies, leading only to minor changes in the spectra of figure 12(b).

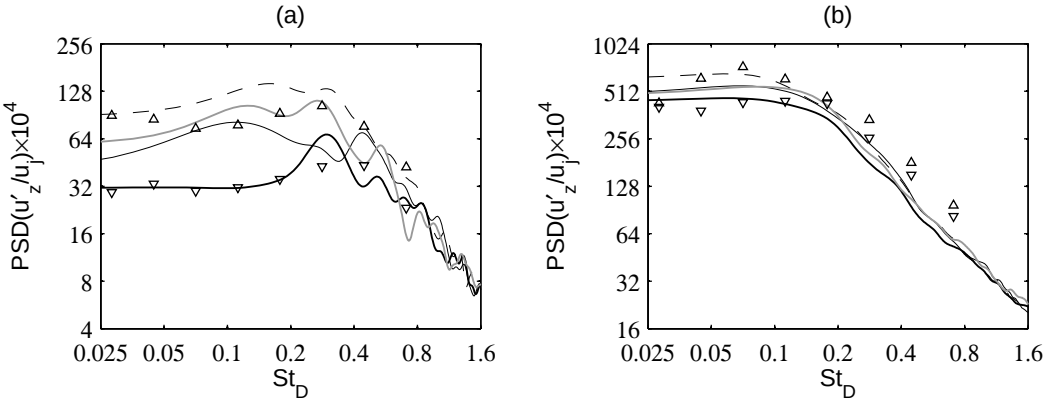

Figure 12. Power spectral densities (PSD) of velocity fluctuations u'_z at $z = z_c$, (a) at $r = 0$ and (b) at $r = r_0$, as functions of St_D, for: ——— $T_j = T_a$ and $\mathrm{Re}_D = 10^5$, ——— $T_j = 1.5T_a$ and $\mathrm{Re}_D = 10^5$, – – – $T_j = 2.25T_a$ and $\mathrm{Re}_D = 10^5$, ——— $T_j = 1.5T_a$ and $\mathrm{Re}_D = 10^5$; measurements of Bridges & Wernet[16] for M = 0.9 jets with $D = 5.1$ cm: ▽ $T_j = 0.84T_a$, △ $T_j = 1.76T_a$.

Turning to the density fields, the centerline rms values of density ρ' are presented in figures 13(a-b).

Unsurprisingly, using a normalization by the ambient density, they increase as temperature varies from $T_j = T_a$ up to $T_j = 2.25T_a$ in figure 13(a). The results of figure 13(b), where a non-dimensionalization by $|\rho_j - \rho_a|$ is applied for the hot jets, are more unexpected. Here, the density rms values begin to rise about $4r_0$ upstream of the end of the potential core, reach a peak at $z \simeq 15r_0$ for the jets at $T_j = 1.5T_a$ and $z \simeq 14r_0$ for the jet at $T_j = 2.25T_a$, and then gradually decrease. In the same way as for the centerline turbulence intensities in figures 11(a-b), the effects of the Reynolds number are negligible. In contrast, however, the intensity of density fluctuations exhibits much sharper growth, a peak location closer to the end of the potential core, namely at $z \simeq z_c + 3r_0$ instead of $z \simeq z_c + 6r_0$, and a maximum value decreasing with temperature, from $11.5 - 11.6\%$ at $T_j = 1.5T_a$ down to 9.9% at $T_j = 2.25T_a$, Moreover, the profile obtained for the jet at $T_j = 2.25T_a$ compares well the experimental data of Panda[18] for a jet at M = 0.9 and $T_j = 2.27T_a$, in particular in its peak region. The measurements nevertheless show an increase in level with the axial distance for $z \geq 16r_0$, which is the case neither in the present simulations, nor in the previous jet LES of Bodony & Lele.[22]

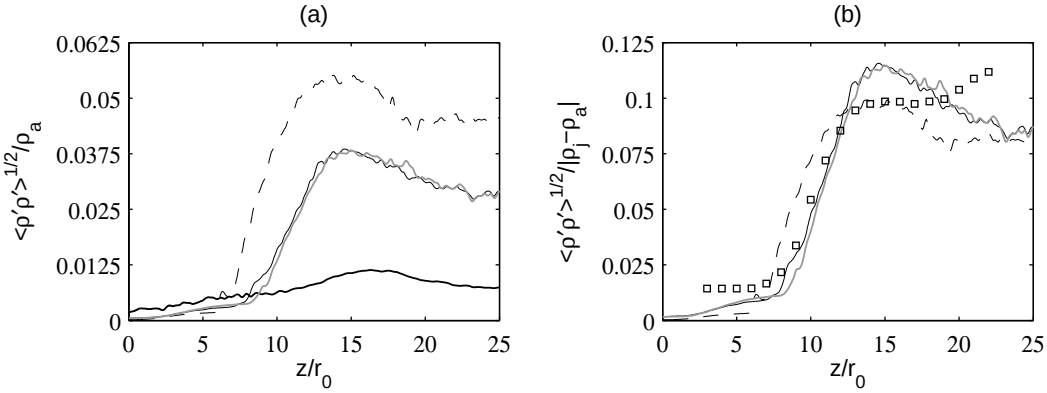

Figure 13. Centerline variations of rms values of density fluctuations ρ', normalized (a) by ρ_a and (b) by $|\rho_j - \rho_a|$, for: ——— $T_j = T_a$ and $\mathrm{Re}_D = 10^5$, ——— $T_j = 1.5T_a$ and $\mathrm{Re}_D = 5 \times 10^4$, – – – $T_j = 2.25T_a$ and $\mathrm{Re}_D = 2.5 \times 10^4$, ——— $T_j = 1.5T_a$ and $\mathrm{Re}_D = 10^5$; □ measurements of Panda[18] for a M = 0.9 jet with $D = 5.1$ cm at $T_j = 2.27T_a$.

Spectra of density ρ' normalized by $|\rho_j - \rho_a|$ are calculated at $z = z_c$ on the centerline and the nozzle lip line of the hot jets, and shown in figures 14(a-b). They are found to be well consistent with data obtained by Panda[18] in a $T_j = 2.7T_a$ jet at axial positions $z = 10r_0$ and $z = 12r_0$, between which the end of the jet potential core most probably lies. Their shapes are similar to those of the velocity spectra of figures 12(a-b) evaluated at identical locations. They also appear not to depend significantly on temperature, in particular at $r = r_0$ in figure 14(b). However, whereas the main effect of jet heating consists in an amplification at low frequencies in the velocity spectra, there seems to be a reduction at high frequencies in the density spectra. This decrease is especially pronounced at $r = 0$ in figure 14(a) for $\mathrm{St}_D \geq 0.4$. In this case, in addition, the peak Strouhal number is around $\mathrm{St}_D = 0.15$, which is slightly lower than those noticed in the velocity spectra.

Considering that links exist[18,48–51] in jet flows between turbulent phenomena on the axis at the end of the potential core and noise generation, the skewness and kurtosis factors of the centerline fluctuations of axial velocity and density are estimated. Due to the difficulty to make high-order correlations converge for relatively short time signals, they show significant oscillations. They are nonetheless presented in figures 15 and 16. In figure 15(a-b), large negative and positive values of skewness and kurtosis, respectively, are found for the centerline velocity fluctuations in all cases for $z \simeq 8r_0 - 15r_0$ with a peak around the position of the end of the potential core. Therefore, intermittency is strong in that region, as expected. It can be attributed to the sudden intrusion of low-velocity vortical structures in the jet core.[49,50] Based on the present LES results, this flow feature appears, in addition, to depend significantly neither on the Reynolds number nor on the jet temperature.

As for the skewness and kurtosis factors of the centerline density fluctuations, in figure 16(a-b), their peak values are small in the isothermal jet, but drastically increase with the temperature in the hot jets. In the isothermal case, moderate values of skewness are however seen around $z = 12r_0$, which can be connected with the burst mentioned above of low-velocity turbulent structures in the potential core at ambient density. In the hot jets, large positive values of skewness strongly emerge around $z = 8r_0$ for $T_j = 1.5T_a$, and $z = 6r_0$

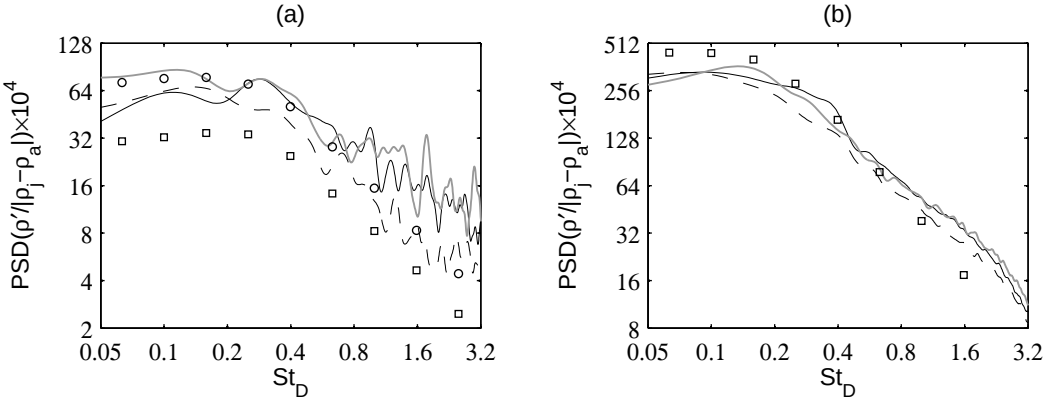

Figure 14. Power spectral densities (PSD) of density fluctuations ρ' at $z = z_c$, (a) at $r = 0$ and (b) at $r = r_0$, as functions of St_D, for: ——— $T_j = 1.5T_a$ and $\mathrm{Re}_D = 10^5$, − − − $T_j = 2.25T_a$ and $\mathrm{Re}_D = 10^5$, ——— $T_j = 1.5T_a$ and $\mathrm{Re}_D = 10^5$; measurements of Panda[18] for a M = 0.9 jet with $D = 5.1$ cm at $T_j = 2.7T_a$: □ at $z = 10r_0$, ○ at $z = 12r_0$.

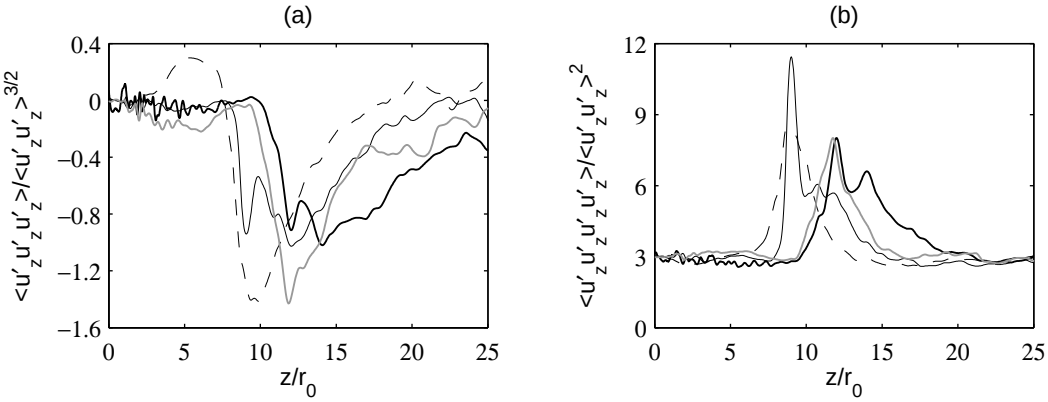

Figure 15. Centerline variations of (a) the skewness and (b) the kurtosis factors of velocity fluctuations u'_z for: ——— $T_j = T_a$ and $\mathrm{Re}_D = 10^5$, ——— $T_j = 1.5T_a$ and $\mathrm{Re}_D = 5 \times 10^4$, − − − $T_j = 2.25T_a$ and $\mathrm{Re}_D = 2.5 \times 10^4$, ——— $T_j = 1.5T_a$ and $\mathrm{Re}_D = 10^5$.

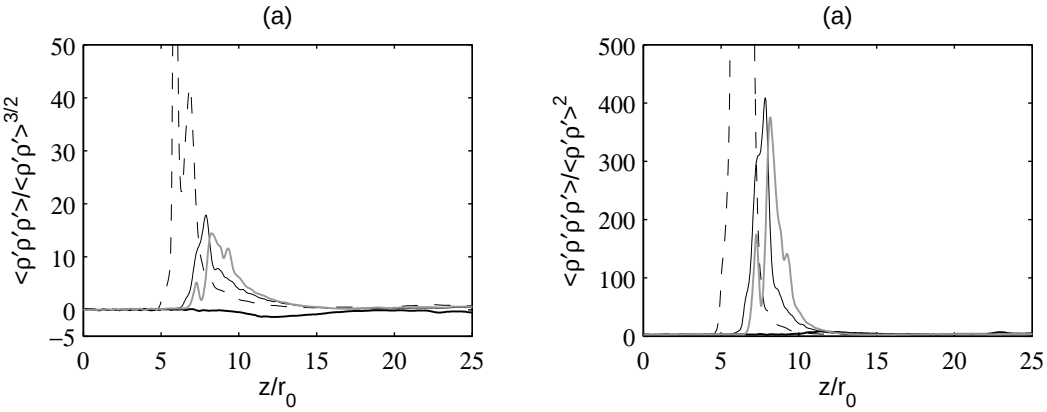

Figure 16. Centerline variations of (a) the skewness and (b) the kurtosis factors of density fluctuations ρ' for: ——— $T_j = T_a$ and $\mathrm{Re}_D = 10^5$, ——— $T_j = 1.5T_a$ and $\mathrm{Re}_D = 5 \times 10^4$, − − − $T_j = 2.25T_a$ and $\mathrm{Re}_D = 2.5 \times 10^4$, ——— $T_j = 1.5T_a$ and $\mathrm{Re}_D = 10^5$.

for $T_j = 2.25T_a$. This is most probably due to the intermittent intrusion of high-density (cold) fluid in the low-density (hot) potential core. What is more surprising is that the maximum intermittency is, contrary to what is obtained for the velocity fluctuations, located well upstream of the end of the potential core at $z \simeq z_c - 5r_0$. This may be of importance regarding noise generation, which will be examined in further studies.

For that purpose, it will be interesting to compute correlations between flow quantities in the jets, including velocity and density, and pressure outside, as was done in several recent experimental and numerical investigations.[18,48,49,52–54] From the present simulation databases, unfortunately, it is difficult to determine converged flow-acoustic correlations due to the limited signal duration. Preliminary results obtained for the hot jet at $T_j = 1.5T_a$ and $\mathrm{Re}_D = 10^5$ are however provided in figures 17(a-b). The cartographies show correlations calculated between the centerline fluctuations of axial velocity and density, and the pressure signal at $z = 24r_0$ and $r = 6.5r_0$. The latter signal is low-pass filtered to damp components with $\mathrm{St}_D \leq 0.2$, which are contaminated by near-field aerodynamic disturbances.[55] Extended regions of high correlation levels are visible upstream of the end of the potential core. Maximum values are located around $z = z_c - r_0$ for the velocity and $z = z_c - 5r_0$ for the density, which correspond to the position of maximum intermittency in the respective flow signals. They are also found close to the time delay given by a propagation at the ambient speed of sound, which supports that the correlations result from the presence of sound sources on the jet axis. Peak correlations are moreover negative for the velocity and positive for the density, as was the case in a previous study for a coaxial hot jet,[52] which can be related to intermittent arrival of low-velocity high-density (cold) fluid in the jet core.

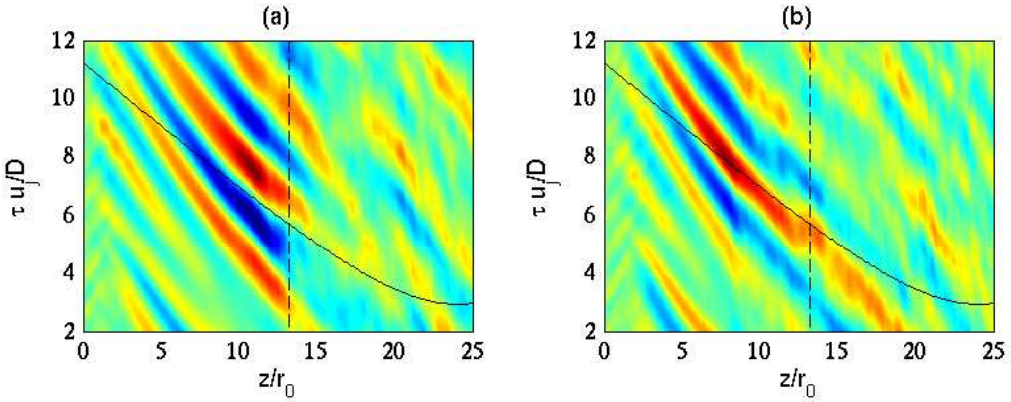

Figure 17. Normalized correlations between the low-pass filtered pressure at $z = 24r_0$ and $r = 6.5r_0$ and the centerline fluctuations of (a) axial velocity and (b) density for the jet at $T_j = 1.5T_a$ and $\mathrm{Re}_D = 10^5$ (τ is the time delay between the signals); ——— time delay for a propagation at the ambient speed of sound, − − − $z = z_c$. The color scale ranges from -0.25 to 0.25.

IV. Conclusion

This paper presents the properties of velocity and density fluctuations in one isothermal and three hot jets at an acoustic Mach number M = 0.9 and Reynolds numbers $2.5 \times 10^4 \leq \mathrm{Re}_D \leq 10^5$ computed using Large-Eddy Simulation in a previous study. Rms values and spectra, as well as skewness and kurtosis factors, are shown, and compared with corresponding experimental data, including those from Bridges & Wernet[15,16] and Panda.[18] Good agrement is found, in particular for the spectra obtained in the shear layers and at $z = z_c$ at the end of the potential.

Concerning the velocity fluctuations, their characteristics are relatively similar in the isothermal jet and in the hot jets. In this case, increasing temperature mainly results in higher overall levels, and stronger low-frequency components, especially at $z = z_c$ on the jet centerline, but the skewness and kurtosis factors do not change much. As for the density fluctuations, their amplitude increases with the temperature, as expected, but above all, they show quite different structures when the jets are heated. In the hot jets, on the contrary to what is found in the isothermal jet, the density shear layer indeed lies outside the velocity shear layer, and large values of skewness and kurtosis are obtained for the density fluctuations, indicating significant intermittency. The implications of these results regarding noise generation in the jets will be explored in

more detail in further works. For that, it could be useful to extend the jet simulations, in order to compute correlations between aerodynamic fluctuations in the jets and the sound pressure radiated outside based on longer time signals.

Acknowledgments

This work was granted access to the HPC resources of CINES (Centre Informatique National de l'Enseignement Supérieur) and IDRIS (Institut du Développement et des Ressources en Informatique Scientifique) under the allocation 2013-2a0204 made by GENCI (Grand Equipement National de Calcul Intensif).

References

[1]Fisher, M.J., Lush, P.A., and Harper-Bourne, M., "Jet noise," *J. Sound Vib.*, Vol. 28, No. 3, 1973, pp. 563-585.

[2]Hoch, R.G., Duponchel, J.P., Cocking, B.J., and Bryce, W.D., "Studies of the influence of density on jet noise," *J. Sound Vib.*, Vol. 28, No. 4, 1973, pp. 649-668.

[3]Tanna, H.K., Dean, P.D., and Fisher, M.J., "The influence of temperature on shock-free supersonic jet noise," *J. Sound Vib.*, Vol. 39, No. 4, 1975, pp. 429-460.

[4]Tanna, H.K., "An experimental study of jet noise. Part I: Turbulent mixing noise," *J. Sound Vib.*, Vol. 50, No. 3, 1977, pp. 405-428.

[5]Bridges, J. and Brown, C.A., "Validation of the small hot jet acoustic rig for aeroacoustics," AIAA Paper 2005-2846, 2005. See also: Brown, C. and Bridges, J., "Small hot jet acoustic rig validation," NASA TM-2006-214234, 2006.

[6]Morfey, C.L., "Amplification of aerodynamic noise by convected flow inhomogeneities," *J. Sound Vib.*, Vol. 31, No. 4, 1973, pp. 391-397.

[7]Tester, B.J. and Morfey, C.L., "Developments in jet noise modelling - Theoretical predictions and comparisons with measured data," *J. Sound Vib.*, Vol. 46, No. 1, 1976, pp. 79-103.

[8]Morfey, C.L., Szewczyk, V.M., and Tester, B.J., "New scaling laws for hot and cold jet mixing noise based on a geometric acoustics model," *J. Sound Vib.*, Vol. 61, No. 2, 1978, pp. 255-292.

[9]Viswanathan, K., "Aeroacoustics of hot jets," *J. Fluid Mech.*, Vol. 516, 2004, pp. 39-82.

[10]Tester, B.J. and Morfey, C.L., "Jet mixing noise: a review of single stream temperature effects," AIAA Paper 2009-3376, 2009.

[11]Harper-Bourne, M., "Jet noise measurements: past and present," *Int. J. of Aeroacoustics*, Vol. 9, No. 4 & 5, 2010, pp. 559-588.

[12]Zaman, K.B.M.Q., "Effect of initial boundary-layer state on subsonic jet noise," *AIAA J.*, Vol. 50, No. 8, 2012, pp. 1784-1795.

[13]Karon, A.Z. and Ahuja, K.K., "Effect of nozzle-exit boundary layer on jet noise," AIAA Paper 2013-0615, 2013.

[14]Lau, J.C., "Effects of exit Mach number and temperature on mean-flow and turbulence characteristics in round jets," *J. Fluid Mech.*, Vol. 105, 1981, pp. 193-218.

[15]Bridges, J. and Wernet, M., "Measurements of the aeroacoustic sound source in hot jets," AIAA Paper 2003-3130, 2003.

[16]Bridges, J. and Wernet, M.P., "Effect of temperature on jet velocity spectra," AIAA Paper 2007-3628, 2007.

[17]Bridges, J., "Effect of heat on space-time correlations in jets," AIAA Paper 2006-2534, 2006.

[18]Panda, J., "Experimental investigation of turbulent density fluctuations and noise generation from heated jets," *J. Fluid Mech.*, Vol. 591, 2007, pp. 73-96.

[19]Colonius, T. and Lele, S.K., "Computational aeroacoustics: progress on nonlinear problems of sound generation," *Progress in Aerospace Sciences*, Vol. 40, 2004, pp. 345-416.

[20]Bailly, C. and Bogey, C., "Contributions of CAA to jet noise research and prediction," *Int. J. Comput. Fluid Dyn.*, Vol. 18, No. 6, 2004, pp. 481-491.

[21]Wang, M., Freund J.B., and Lele, S.K., "Computational prediction of flow-generated sound," *Annu. Rev. Fluid. Mech.*, Vol. 38, 2006, pp. 483-512.

[22]Bodony, D.J. and Lele, S.K., "On using large-eddy simulation for the prediction of noise from cold and heated turbulent jets," *Phys. Fluids*, Vol. 17, No. 8, 2005, 085103.

[23]Bogey, C. and Marsden, O., "Numerical investigation of temperature effects on properties of subsonic turbulent jets," *19th AIAA/CEAS Aeroacoustics Conference*, 27-29 May 2013, AIAA Paper 2013-2140.

[24]Bogey, C., Marsden, O., and Bailly, C., "Large-Eddy Simulation of the flow and acoustic fields of a Reynolds number 10^5 subsonic jet with tripped exit boundary layers," *Phys. Fluids*, Vol. 23, No. 3, 2011, 035104.

[25]Bogey, C., Marsden, O., and Bailly, C., "On the spectra of nozzle-exit velocity disturbances in initially nominally turbulent jets," *Phys. Fluids*, Vol. 23, No. 9, 2011, 091702.

[26]Bogey, C., Marsden, O., and Bailly, C., "Influence of initial turbulence level on the flow and sound fields of a subsonic jet at a diameter-based Reynolds number of 10^5," *J. Fluid Mech.*, Vol. 701, 2012, pp. 352-385.

[27]Bogey, C., Marsden, O., and Bailly, C., "Effects of moderate Reynolds numbers on subsonic round jets with highly disturbed nozzle-exit boundary layers," *Phys. Fluids*, Vol. 24, No. 10, 2012, 105107.

[28]Bogey, C. and Marsden, O., "Identification of the effects of the nozzle-exit boundary-layer thickness and its corresponding Reynolds number in initially highly disturbed subsonic jets," *Phys. Fluids*, Vol. 25, No. 5, 2013, 055113.

[29]Bogey, C. and Bailly, C., "Influence of nozzle-exit boundary-layer conditions on the flow and acoustic fields of initially laminar jets," *J. Fluid Mech.*, Vol. 663, 2010, pp. 507-539.

[30]Zaman, K.B.M.Q., "Effect of initial condition on subsonic jet noise," *AIAA J.*, Vol. 23, 1985, pp. 1370-1373.

[31]Zaman, K.B.M.Q., "Far-field noise of a subsonic jet under controlled excitation," *J. Fluid Mech.*, Vol. 152, 1985, pp. 83-111.

[32]Mohseni, K. and Colonius, T., "Numerical treatment of polar coordinate singularities," *J. Comput. Phys.*, Vol. 157, No. 2, 2000, pp. 787-795.

[33]Bogey, C., de Cacqueray, N., and Bailly, C., "Finite differences for coarse azimuthal discretization and for reduction of effective resolution near origin of cylindrical flow equations," *J. Comput. Phys.*, Vol. 230, No. 4, 2011, pp. 1134-1146.

[34]Bogey, C. and Bailly, C., "A family of low dispersive and low dissipative explicit schemes for flow and noise computations," *J. Comput. Phys.*, Vol. 194, No. 1, 2004, pp. 194-214.

[35]Bogey, C., de Cacqueray, N., and Bailly, C., "A shock-capturing methodology based on adaptative spatial filtering for high-order non-linear computations," *J. Comput. Phys.*, Vol. 228, No. 5, 2009, pp. 1447-1465.

[36]Berland, J., Bogey, C., Marsden, O., and Bailly, C., "High-order, low dispersive and low dissipative explicit schemes for multi-scale and boundary problems," *J. Comput. Phys.*, Vol. 224, No. 2, 2007, pp. 637-662.

[37]Tam, C.K.W and Dong, Z., "Radiation and outflow boundary conditions for direct computation of acoustic and flow disturbances in a nonuniform mean flow., *J. Comput. Acoust.*, Vol. 4, No. 2,, 1996, pp. 175201.

[38]Bogey, C. and Bailly, C., "Three-dimensional non reflective boundary conditions for acoustic simulations: far-field formulation and validation test cases," *Acta Acustica*, Vol. 88, No. 4, 2002, pp. 463-471.

[39]Bogey, C. and Bailly, C., "Large Eddy Simulations of transitional round jets: influence of the Reynolds number on flow development and energy dissipation," *Phys. Fluids*, Vol. 18, No. 6, 2006, 065101.

[40]Bogey, C. and Bailly, C., "Turbulence and energy budget in a self-preserving round jet: direct evaluation using large-eddy simulation," *J. Fluid Mech.*, Vol. 627, 2009, pp. 129-160.

[41]Fauconnier, D., Bogey, C., and Dick, E., "On the performance of relaxation filtering for large-eddy simulation," *J. Turbulence*, Vol. 14, No. 1, 2013, pp. 22-49.

[42]Michalke, A., "Survey on jet instability theory," *Prog. Aerospace Sci.*, Vol. 21, 1984, pp. 159-199.

[43]Gutmark, E. and Ho, C.-M., "Preferred modes and the spreading rates of jets," *Phys. Fluids*, Vol. 26, No. 10, 1983, pp. 2932-2938.

[44]Lepicovsky, J., "Experimental research on mixing enhancement in heated free jet flows," *3rd ASME/JSME Joint Fluids Engineering Conference*, 18-23 July 1999, San Francisco, CA, USA, No. FEDSM99-7247.

[45]Kearney-Fischer, M., Kim, J.-H., and Samimy, M., "Control of a high Reynolds number Mach 0.9 heated jet using plasma actuators," *Phys. Fluids*, Vol. 21, No. 9, 2009, 095101.

[46]Fleury, V., Bailly, C., Jondeau, E., Michard, M., and Juvé, D., "Space-time correlations in two subsonic jets using dual-PIV measurements," *AIAA J.*, Vol. 46, No. 10, 2008, pp. 2498-2509.

[47]Arakeri, V.H., Krothapalli, A., Siddavaram, V., Alkislar, M.B., and Lourenco, L., "On the use of microjets to suppress turbulence in a Mach 0.9 axisymmetric jet," *J. Fluid Mech.*, Vol. 490, 2003, pp. 75-98.

[48]Panda, J., Seasholtz, R.G., and Elam, K.A., "Investigation of noise sources in high-speed jets via correlation measurements," *J. Fluid Mech.*, Vol. 537, 2005, pp. 349-385.

[49]Bogey, C. and Bailly, C., "An analysis of the correlations between the turbulent flow and the sound pressure field of subsonic jets," *J. Fluid Mech.*, Vol. 583, 2007, pp. 71-97.

[50]Bogey, C., Bailly, C., and Juvé, D., "Noise investigation of a high subsonic, moderate Reynolds number jet using a compressible LES," *Theoret. Comput. Fluid Dynamics*, Vol. 16, No. 4, 2003, pp. 273-297.

[51]Tam, C.K.W., Viswanathan, K., Ahuja, K.K., and Panda, J., "The sources of jet noise: experimental evidence," *J. Fluid Mech.*, Vol. 615, 2008, pp. 253-292.

[52]Bogey, C., Barré, S., Juvé, D., and Bailly, C., "Simulation of a hot coaxial jet : direct noise prediction and flow-acoustics correlations," *Phys. Fluids*, Vol. 21, No. 3, 2009, 035105.

[53]Grizzi, S and Camussi, R., "Wavelet analysis of near-field pressure fluctuations generated by a subsonic jet," *J. Fluid Mech.*, Vol. 698, 2012, pp. 93-124.

[54]Henning, A., Koop, L., and Schröder, A., "Causality correlation analysis on a cold jet by means of simultaneous Particle Image Velocimetry and microphone measurements," *J. Sound Vib.*, Vol. 332, 2013, pp. 3148-3162.

[55]Arndt, R.E.A, Long, D.F., and Glauser, M.N., "The proper orthogonal decomposition of pressure fluctuations surrounding a turbulent jet," *J. Fluid Mech.*, Vol. 340, 1997, pp. 1-33.